Metathesis Activity Encoded in the Metallacyclobutane Carbon-13 NMR Chemical Shift Tensors

Christopher P. Gordon, Keishi Yamamoto, Wei-Chih Liao, Florian Allouche, Richard A. Andersen, Christophe Copéret, Christophe Raynaud, Odile Eisenstein

▶ **To cite this version:**

Christopher P. Gordon, Keishi Yamamoto, Wei-Chih Liao, Florian Allouche, Richard A. Andersen, et al.. Metathesis Activity Encoded in the Metallacyclobutane Carbon-13 NMR Chemical Shift Tensors. ACS Central Science, 2017, 3 (7), pp.759-768. 10.1021/acscentsci.7b00174 . hal-01569539

HAL Id: hal-01569539
https://hal.science/hal-01569539

Submitted on 25 May 2021

HAL is a multi-disciplinary open access archive for the deposit and dissemination of scientific research documents, whether they are published or not. The documents may come from teaching and research institutions in France or abroad, or from public or private research centers.

L'archive ouverte pluridisciplinaire **HAL**, est destinée au dépôt et à la diffusion de documents scientifiques de niveau recherche, publiés ou non, émanant des établissements d'enseignement et de recherche français ou étrangers, des laboratoires publics ou privés.

This is an open access article published under an ACS AuthorChoice License, which permits copying and redistribution of the article or any adaptations for non-commercial purposes.

ACS central science

Research Article

http://pubs.acs.org/journal/acscii

Metathesis Activity Encoded in the Metallacyclobutane Carbon-13 NMR Chemical Shift Tensors

Christopher P. Gordon,[†,#] Keishi Yamamoto,[†,#] Wei-Chih Liao,[†] Florian Allouche,[†] Richard A. Andersen,[*,‡] Christophe Copéret,[*,†] Christophe Raynaud,[*,§] and Odile Eisenstein[*,§,∥]

[†]Department of Chemistry and Applied Biosciences, ETH Zürich, Vladimir Prelog Weg 1-5, 8093, Zürich, Switzerland

[‡]Department of Chemistry, University of California, Berkeley, California 94720, United States

[§]Institut Charles Gerhardt, UMR 5253 CNRS-Université de Montpellier, Université de Montpellier, 34095 Montpellier, France

[∥]Centre for Theoretical and Computational Chemistry (CTCC), Department of Chemistry, University of Oslo, P.O. Box 1033, Blindern, 0315 Oslo, Norway

Supporting Information

ABSTRACT: Metallacyclobutanes are an important class of organometallic intermediates, due to their role in olefin metathesis. They can have either planar or puckered rings associated with characteristic chemical and physical properties. Metathesis active metallacyclobutanes have short M−$C_{\alpha/\alpha'}$ and M···C_β distances, long $C_{\alpha/\alpha'}$−C_β bond length, and isotropic ^{13}C chemical shifts for both early d^0 and late d^4 transition metal compounds for the α- and β-carbons appearing at ca. 100 and 0 ppm, respectively. Metallacyclobutanes that do not show metathesis activity have ^{13}C chemical shifts of the α- and β-carbons at typically 40 and 30 ppm, respectively, for d^0 systems, with upfield shifts to ca. −30 ppm for the α-carbon of metallacycles with higher d^n electron counts (n = 2 and 6). Measurements of the chemical shift tensor by solid-state NMR combined with an orbital (natural chemical shift, NCS) analysis of its principal components ($\delta_{11} \geq \delta_{22} \geq \delta_{33}$) with two-component calculations show that the specific chemical shift of metathesis active metallacyclobutanes originates from a low-lying empty orbital lying in the plane of the metallacyclobutane with local π^*(M−$C_{\alpha/\alpha'}$) character. Thus, in the metathesis active metallacyclobutanes, the α-carbons retain some residual alkylidene character, while their β-carbon is shielded, especially in the direction perpendicular to the ring. Overall, the chemical shift tensors directly provide information on the predictive value about the ability of metallacyclobutanes to be olefin metathesis intermediates.

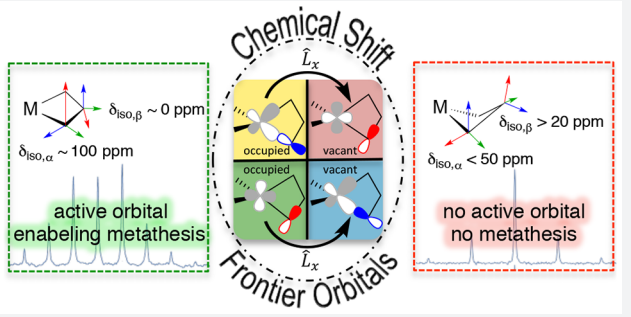

INTRODUCTION

Olefin metathesis is an efficient process to make carbon−carbon bonds and has been increasingly used in academia and industry to build molecules, from simple chemicals like propene to polymers and complex building blocks for natural products like hepatitis C drugs.[1−8] This reaction is catalyzed by transition-metal (M) complexes bearing an alkylidene ligand (**M-ene**), through a [2 + 2]-cycloaddition with an olefin to generate a metallacyclobutane (the Chauvin mechanism).[9,10] Density functional theory (DFT) calculations have shown that metallacyclobutanes with a trigonal bipyramidal geometry (**M-TBP**) are the key intermediates in metathesis for d^0 Schrock alkylidene catalysts[11−16] — compounds with the general structure (X)(Y)M(E)(=CHR) with M(E) = Ta(OAr), Mo(=NR), W(=NR), W(=O), Re(≡CR) (Scheme 1A).[17−20] The corresponding square-pyramidal (**M-SP**) isomeric structures are known, but they are not on the metathesis reaction pathway and correspond to off-cycle resting states. The general structural features of the **M-TBP** compounds (M = Ta, Mo, W, and Re) differ from the **M-SP** isomers as follows:[11−16,21−30] (i) the M−C_α−C_β−$C_{\alpha'}$ torsion angles ξ are close to 0° in **M-TBP**, but deviate significantly from 0° for the **M-SP** isomers, (ii) the M−$C_{\alpha/\alpha'}$ and M···C_β distances are shortened, while the $C_\alpha(C_{\alpha'})$−C_β bond distances are elongated in the **M-TBP** relative to the **M-SP** isomers, and (iii) the ^{13}C isotropic chemical shifts (δ_{iso}) for the α- and β-carbons are ca. 100 and 0 ppm, respectively in **M-TBP**, while they are at ca. 40 and 30 ppm, respectively, in **M-SP** (Scheme 1). Similar NMR signatures have been found in well-defined silica-supported metathesis catalysts,[31−33] based on d^0 tungsten imido and oxo metallacyclobutanes, (≡SiO)(X)W(E)($CH_2CH_2CH_2$) (E = NAr or O, X = 2,5-dimethylpyrrolate,[34] alkoxides,[35−39] or thiolates[40,41]) or the alumina-supported CH_3ReO_3-catalysts (Scheme 1B)[42] and have been used to distinguish TBP and SP structures. Molecular Ru-based metathesis catalysts also involve pentacoordinated TBP metallacyclobutanes as key reaction intermediates, albeit with a d^4 configuration (**Ru-TBP**, Scheme 1C).[43−49] They show similar structures and NMR features as the d^0 TBP

Received: April 21, 2017
Published: June 14, 2017

Downloaded via UNIV MONTPELLIER on May 25, 2021 at 07:40:54 (UTC).
See https://pubs.acs.org/sharingguidelines for options on how to legitimately share published articles.

© 2017 American Chemical Society

DOI: 10.1021/acscentsci.7b00174
ACS Cent. Sci. 2017, 3, 759−768

Scheme 1. (A–E) Active and Inactive Metallacyclobutanes Are Shown in Green and Red Boxes, Respectively, with Their ^{13}C NMR Chemical Shifts[a]

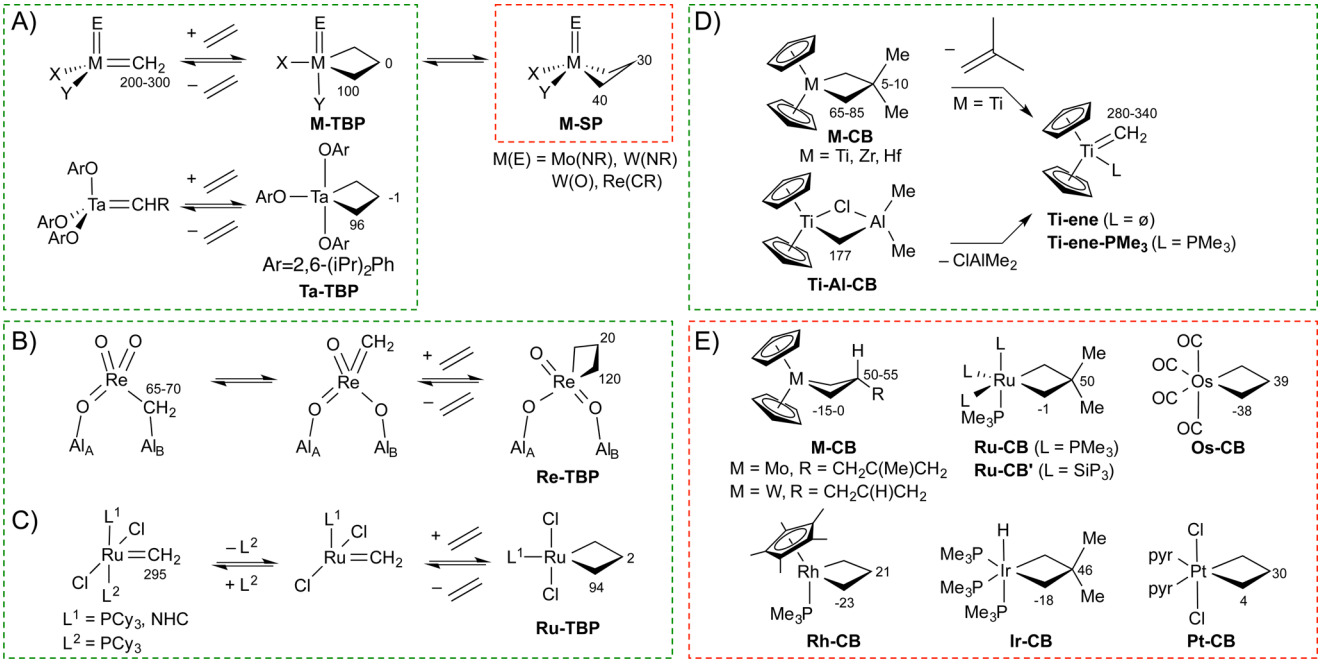

[a](A) Metallacyclobutanes (Mo, W, Re, and Ta) derived from Schrock alkylidenes; (B) alumina-supported $MeReO_3$; (C) Ru(IV) systems; (D) Group IV metallacyclobutanes, and (E) metallacyclobutanes with no reported metathesis activity: **M-CB** for M = Mo, W, Ru (L = PMe_3 or L_3 = SiP_3 = $(PMe_2CH_2)_3SiMe$), Os, Rh, Ir, and Pt).

homologues outlined above. However, in these cases, the SP isomer is unknown and is calculated to be at high energy.[50] One of the first olefin metathesis catalysts, which demonstrated the validity of the Chauvin mechanism,[9,10] is the d^0 bis-cyclopentadienyltitanacyclobutane, $Cp_2Ti(CH_2CMe_2CH_2)$ (**Ti-CB**, Scheme 1D) derived from the Tebbe reagent $Cp_2Ti(CH_2AlMe_2Cl)$ (**Ti–Al–CB**).[51−55] This metathesis active metallacyclobutane shows ^{13}C chemical shifts similar to those obtained for the **M-TBP** species mentioned above with α- and β-carbons at 81 and 6 ppm, respectively.[56,57] Similar chemical shifts, albeit being significantly lower for the α-carbons, have also been observed for the Cp_2Zr and Cp_2Hf metallacyclobutane derivatives.[58] Several other metallacyclobutanes (**M-CB**) exist, for which no metathesis activity has been reported. The d^2 Mo/W systems $Cp_2M(CH_2CHRCH_2)$ (**Mo-CB**, R = methallyl and **W-CB**, R = allyl)[59,60] and d^6 octahedral $L_4M(CH_2CR_2CH_2)$ systems (**Ru-CB** and **Ru-CB′**, R = Me,[61,62] **Os-CB**, R = H,[63] **Rh-CB**, R = H,[64] **Ir-CB**, R = Me,[65] and **Pt-CB**, R = H[66−68]) display β-carbons at ca. 30−40 ppm and strongly shielded α-carbons, typically <0 ppm (see red box in Scheme 1E).

The data summarized in Scheme 1 implicate an empirical correlation between chemical shift, structure, and activity of the metallacyclobutane in metathesis. The metathesis active metallacyclobutanes display particularly deshielded and shielded α- and β-carbon chemical shifts, respectively, and all have a planar structure (shown in green boxes in Scheme 1). In contrast, metallacyclobutanes with no known metathesis activity display more classical chemical shifts (red box in Scheme 1). The focus of this article is to develop a model that rationalizes the empirical correlation. The isotropic chemical shift (δ_{iso}) is an average of the three principal components of the chemical shift tensor ($\delta_{11} \geq \delta_{22} \geq \delta_{33}$), which individually provide a detailed understanding of the electronic structure of the probe nuclei.[69] They are readily measured by solid-state NMR, calculated with reasonable precision by DFT calculations, and analyzed by a natural chemical shift (NCS) method.[70−97] The corresponding shielding (σ_{ii}, eq 2) can be decomposed into diamagnetic (σ_{dia}, leading to shielding) and paramagnetic plus spin−orbit ($\sigma_{para+SO}$, leading in general to deshielding) terms (eq 3). The differences between spin−orbit and spin-free ZORA calculations are small for alkylidene complexes.[70] In the case of metallacyclobutanes, good results were obtained with scalar relativistic (spin-free) calculations.[16] Consequently, while the calculations include the spin−orbit term, the results can be analyzed by considering only the paramagnetic contribution (eq 4). As a consequence, $\sigma_{para+SO}$ will be written as σ_{para} for convenience. The paramagnetic term along one of its three principal axes i, where $i = x, y$, and z, is associated with the coupling between occupied and empty orbitals of appropriate symmetry by way of the angular momentum operator $\hat{L}_i$ (eq 4) with a determining role of the frontier orbitals that are closer in energy.[69]

In this article, we investigate the origin of the ^{13}C NMR chemical shifts in a series of metallacyclobutanes by evaluation and analysis of their principal components and develop the correlation between ^{13}C chemical shifts and olefin metathesis reactivity by a combination of solid-state NMR experiments and two-component calculations.

$$\delta_{iso} = \frac{1}{3}(\delta_{11} + \delta_{22} + \delta_{33}) \quad (1)$$

$$\delta_{ii} = \sigma_{iso}^{ref} - \sigma_{ii} \quad (i = 1, 2, 3) \quad (2)$$

$$\sigma = \sigma_{dia} + \sigma_{para+SO} \quad (3)$$

$$\sigma_{ii,para} \propto \frac{\langle \Psi_{vac}|\hat{L}_i|\Psi_{occ}\rangle\langle \Psi_{vac}|\hat{L}_i/r^3|\Psi_{occ}\rangle}{\Delta E_{vac-occ}} \quad (4)$$

DOI: 10.1021/acscentsci.7b00174
ACS Cent. Sci. 2017, 3, 759−768

Table 1. Calculated Isotropic Chemical Shifts (δ_{iso}), Principal Components (δ_{ii}) and Span (Ω) of the Chemical Shift Tensor for Selected Metallacyclobutanes (Experimental Values Are Given in Parentheses When Available)[a]

Entry	Compound	Site	δ_{iso}	δ_{11}	δ_{22}	δ_{33}	$\Omega = \delta_{11} - \delta_{33}$
1	W-TBP[b]	α–C	102 (102)	222 (222)	59 (42)	25 (41)	197 (181)
		β–C	−6 (−7)	31 (30)	−7 (21)	−41 (−71)	72 (101)
2	Ti-CB	α–C[d]	81 (81)	161 (161)	76 (78)	6 (5)	155 (156)
		β–C	6 (6)	39 (44)	21 (19)	−43 (−46)	82 (90)
3	Ti-Al-CB	$TiCH_2Al$	187 (177)	469 (419)	94 (102)	−2 (11)	471 (407)
4	Ti-ene-PMe_3	α–C	309 (286)	754 (714)	155 (82)	17 (70)	737 (644)
5	Ti-ene	α–C	338	821	176	18	803
6	Ru-TBP[c]	α–C	100 (94)[e, 43]	218	96	−13	231
		β–C	1 (2)[e, 43]	41	−10	−27	68
7	W-SP[b]	α–C	44	66	46	20	46
		β–C	26	33	29	16	17
8	Mo-CB	α–C	−3 (−8)[e, 60]	35	−6	−37	72
		β–C	49 (50)[e, 60]	90	39	19	71
9	Ru-CB	α–C	3 (−1)	59 (40)	−19 (0)	−31 (−44)	90 (84)
		β–C	48 (50)	85 (91)	32 (31)	27 (27)	58 (64)

[a]Experimental carbon chemical shift tensors are determined by fitting the observed spinning side bands. [b]Ligands: X = $OC(CF_3)_3$, Y = OSi≡, E = NAr and [c]L^1 = H_2IMes (see Scheme 1 and Supporting Information Scheme S1). [d]A second signal with a similar chemical shift tensor is also observed (δ_{iso} = 87 ppm with δ_{11} = 172, δ_{22} = 83, and δ_{33} = 6 ppm). [e]Isotropic chemical shift obtained in solution.

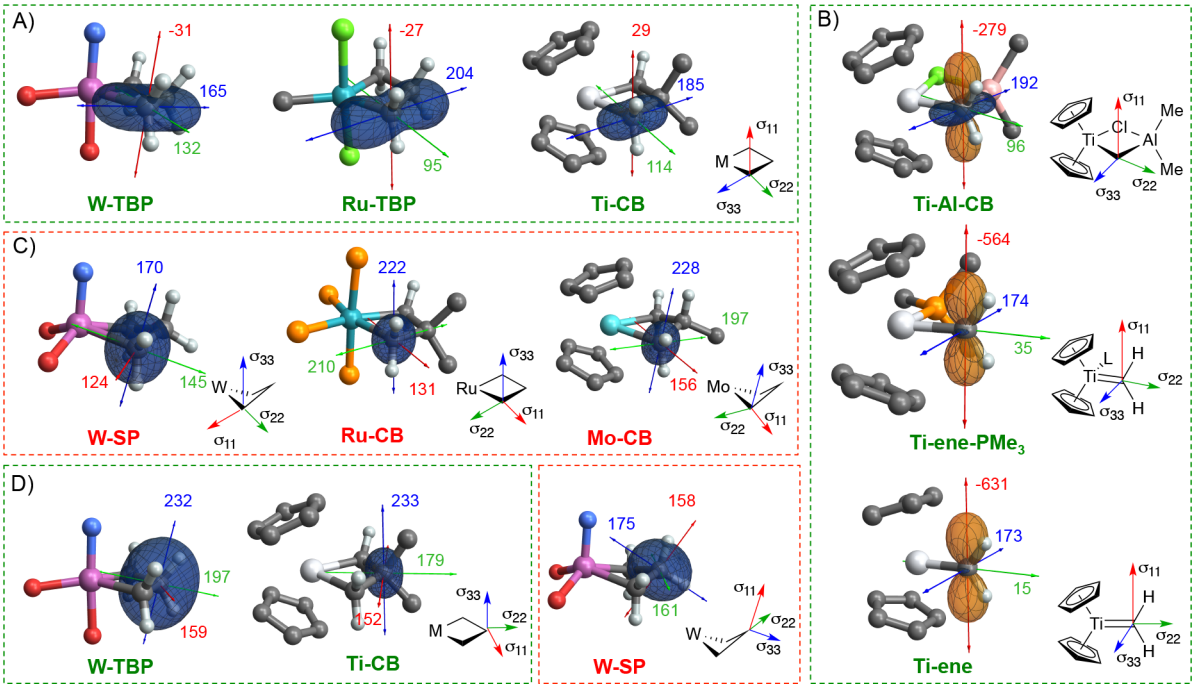

Figure 1. Shielding tensors for the α-carbon of metallacyclobutanes and related alkylidenes: (A) **M-TBP** and **Ti-CB**, (B) **Ti-Al-CB**, **Ti-ene**, and **Ti-ene-PMe_3**. (C) **W-SP**, **Ru-CB**, and **Mo-CB**. (D) Shielding tensors for the β-carbons in **W-TBP**, **Ti-CB**, and **W-SP** (for other systems see Figure S11). The corresponding chemical shift tensor ($\delta_{ii} = \sigma_{ref} - \sigma_{ii}$, eq 2) is oriented in the same way. Compounds for which metathesis activity has been reported are enclosed within green boxes.

RESULTS

Measured and Calculated Principal Components of a Series of Representative Metallacyclobutanes. While there is a large body of literature on isotropic chemical shift values (δ_{iso}), the measurement of the principal components — $\delta_{11} \geq \delta_{22} \geq \delta_{33}$ — of the chemical shifts in organometallic compounds are rare,[78,83,86,89,95] even though these data are readily accessible by solid-state NMR. We have recently measured these values for well-defined silica-supported tungsten catalysts (Table 1, Entries 1 and 7),[39] which are isoelectronic with the corresponding molecular complexes and show similar δ_{iso} values, allowing one to distinguish between TBP and SP metallacyclobutane isomers.[34−39] Additionally, the principal components of selected known complexes — **Ti-CB**, **Ti−Al−CB** and the corresponding stable alkylidene $Cp_2Ti(=CH_2)(PMe_3)$ (**Ti-ene-PMe_3**) as well as **Ru-CB** (Table 1, Entries 2−4 and 9; see also Scheme 1) — have been measured. The principal components of the shielding tensors have been calculated with two-component DFT calculations for all the aforementioned complexes as well as for the putative **Ti-ene** (Entry 5), **Ru-TBP** (Entry 6), which is only known in solution, and **Mo-CB** (Entry 8) (see Supporting Information for computational details). Additional structures with known isotropic chemical shifts have been calculated for **Zr/Hf-CB**, **W-CB**, **Ta-TBP**, **Mo-TBP**, **Mo-SP**, **Os-CB**, **Rh-CB**, **Ir-CB**, and **Pt-CB** (Scheme 1 and Table S1). In all cases,

DOI: 10.1021/acscentsci.7b00174
ACS Cent. Sci. 2017, 3, 759−768

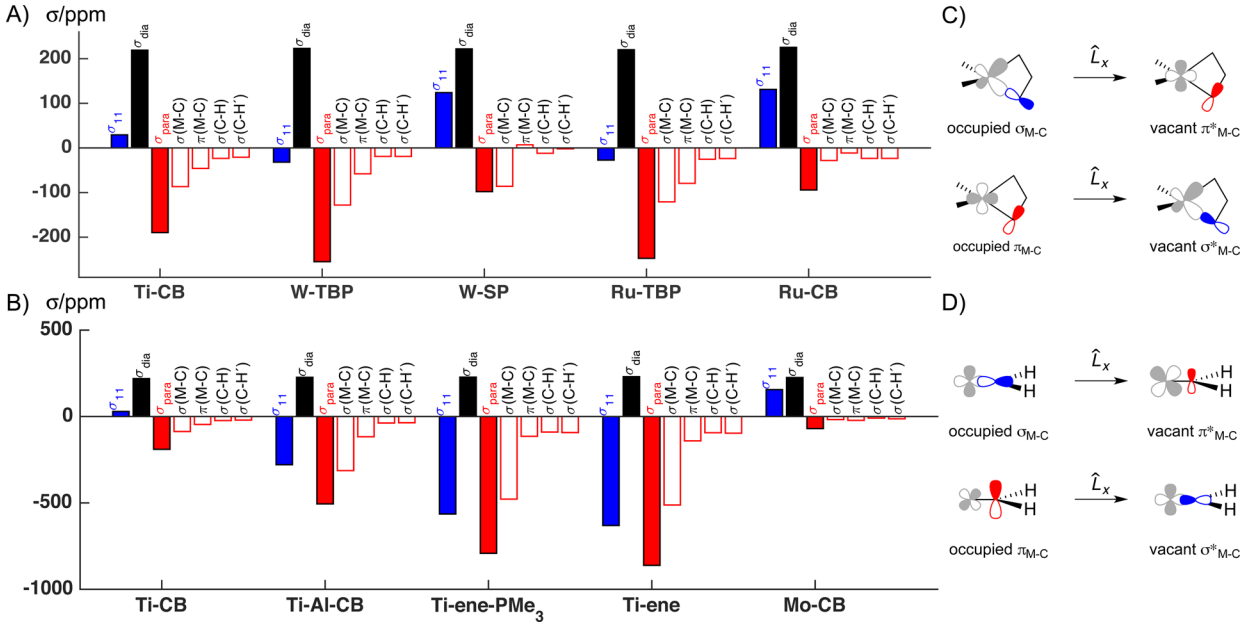

Figure 2. Calculated values of σ_{11}, σ_{dia}, and σ_{para} and decomposition of σ_{para} into its most relevant components by NCS analysis. (A) α-Carbons of various active (**Ti-CB**, **W-TBP**, **Ru-TBP**) and inactive (**W-SP**, **Ru-CB**) metallacyclobutanes. (B) Comparison of **Ti-CB**, **Ti−Al−CB**, related alkylidenes (**Ti-ene-PMe$_3$** and **Ti-ene**) and inactive **Mo-CB**. Note the different scales used in graphs A and B. Orbital interactions determining the deshielding of δ_{11} in (C) metallacyclobutanes and (D) alkylidenes.

experimental and computed values agree reasonably well for δ_{iso} and the principal components (δ_{11}, δ_{22}, and δ_{33}), when available. Overall, the data show that, of the various metallacyclobutanes, the metathesis active catalysts — all **M-TBP** and **Ti-CB** — have deshielded α-carbons and shielded β-carbons at ca. 100 and 0 ppm, respectively. In inactive metallacyclobutanes (**M-SP**, **Ru-CB**, **Mo-CB**, and other metallacyclobutanes of Table S1), the chemical shifts are in the range of 30−40 ppm for α- and β-carbons in most cases, with a few cases having very shielded α-carbons around 0 ppm or below.

In all active metallacyclobutanes (**M-TBP** and **Ti-CB**), the α-carbon is highly anisotropic as evidenced by the significant differences between δ_{11} and δ_{33} (also called span, Ω).[72] In particular, δ_{11} and δ_{22} are deshielded for the α-carbon in comparison with those of the β-carbon. These findings are in contrast with the observation that inactive metallacycles — **M-SP** and other **M-CB** (M = Mo, W, Os, Rh, Ir, and Pt) — show fairly isotropic principal components for both α- and β-carbons, i.e., small Ω, typical of sp^3-carbons (Figure 1, Tables 1 and S2). The orientation of the chemical shift tensor for the α-carbon of all **M-TBP** and **Ti-CB** is similar, with δ_{11} oriented perpendicularly to the plane of the metallacyclobutane, δ_{33} oriented along the C$_\alpha$−C$_\beta$ bond (and essentially perpendicularly to M−C$_\alpha$), and δ_{22} perpendicular to the other two components (Figure 1A). This orientation is the same as in metal carbenes and alkylidenes (illustrated for the Cp$_2$Ti species in Figure 1B).[70,71,98] Similarly, the tensor in **Ti-Al-CB** is oriented as in **Ti-CB**, but with a more deshielded δ_{11} component. This component is further deshielded in **Ti-ene-PMe$_3$** and **Ti-ene**, and oriented perpendicularly to the σ- and π-metal−carbon bonds as found for any alkylidene complex.[70,71] The coordinated PMe$_3$ ligand does not alter the orientation of the shielding tensor (Figure 1B). In contrast, for **M-SP**, **Ru-CB**, and **Mo-CB** — compounds with no reported olefin metathesis activity — the shielded α-carbons have a small anisotropy and are associated with δ_{11} and δ_{22} in the plane of the metallacyclobutane (Figure 1C).

The β-carbon in **Ti-CB** and all **M-TBP** structures has δ_{11} in the plane of the metallacyclobutane and perpendicular to the M−C$_\beta$ axis. The most shielded component (δ_{33}) is now perpendicular to the plane of the metallacycle and δ_{22} is perpendicular to the other two components. This contrasts with the orientation of the chemical shift tensor in metathesis inactive metallacyclobutanes (**M-SP**, **Ru-CB**, and **Mo-CB**; Figures 1D and S11), in which δ_{11} at C$_\beta$ is roughly perpendicular to the average ring plane. For these structures, the tensors at the β-carbon are nearly isotropic (Figure 1D).

NCS Analysis of the Principal Components of the Shielding. To analyze the prior results, a localized orbital analysis, named natural chemical shift (NCS) analysis,[73−76] of the shielding is developed (see eq 2 for relation between shielding σ and chemical shift δ). The σ_{dia} and σ_{para} terms are evaluated for the α- and β-carbons in the various systems discussed above (Figure 2 and Tables S3−S6 and Figures S5−S10). The σ_{dia} term is similar for all carbons of all metallacyclobutanes, **Ti−Al−CB** as well as **Ti-ene** complexes. In contrast, the σ_{para} term greatly differs between α- and β-carbons of **M-TBP** and **Ti-CB**. This effect is most pronounced for σ_{11} and also to a lesser extent for σ_{22}. For other structures (**M-SP**, **Mo/W-CB**, and **Ru-CB**), σ_{para} is rather small, showing again the special character of the α-carbon in **M-TBP** and **Ti-CB**. The determining role of $\sigma_{11,para}$ is particularly evident when considering **Ti−Al−CB**, **Ti-ene-PMe$_3$**, and **Ti-ene**.

The NCS analysis of σ_{11} for the α-carbon of **M-TBP** and **Ti-CB** shows that π(M−C) and σ(M−C) are involved, via the coupling with σ^*(M−C) and π^*(M−C), respectively, through $\hat{L}_x$ (Figure 2 and Table S4; see Figure 2C for naming convention of orbitals). For σ_{22}, deshielding mainly arises from a coupling of σ(C−H) with σ^*(M−C) and π^*(M−C) through $\hat{L}_y$ (Table S5), while the small deshielding in σ_{33} is mostly due to a coupling of σ(M−C) with σ^*(C−H) through $\hat{L}_z$ (Table S5). For **Ti−Al−CB**, the larger deshielding of σ_{11} results from the more efficient coupling of σ(M−C) and π(M−C) with π^*(M−C) and σ^*(M−

DOI: 10.1021/acscentsci.7b00174
ACS Cent. Sci. 2017, 3, 759−768

C), respectively, as expected by substituting a carbon by Al. The similarities in the NMR and NCS fingerprints of **Ti-CB**, **Ti−Al−CB**, **Ti-ene-PMe$_3$**, and **Ti-ene**,[71] also pertain to all **M-TBP** compounds, emphasizing the alkylidene character of the α-carbons in metathesis active metallacyclobutanes (Figure 2A,B).

In all metathesis-active metallacyclobutanes (**M-TBP** and **Ti-CB**), the β-carbon is strongly shielded with $\delta_{iso} \sim 0$ ppm. The shielding mainly results from σ_{dia} that is not significantly compensated by paramagnetic contributions, which are small for σ_{11} and σ_{22}, and essentially null or even slightly positive for σ_{33} (Figure 1D and Tables S2−S3).

The NCS analysis also highlights the difference between active and inactive metallacyclobutanes: the contribution of σ_{para} at the α-carbon is significantly smaller in **W-SP** than in **W-TBP** and does not differ significantly between the α- and β-carbons. All bonds on the α- and β-carbons contribute rather weakly to deshielding, consistent with the absence of low-lying empty orbitals. Similar situations are found in **Ru-CB** and **Mo-CB**.

DISCUSSION

Inspection of the data in Tables 1 and S1 shows a correlation between chemical shift, structure of the M−C$_\alpha$−C$_\beta$−C$_{\alpha'}$ ring and metathesis activity. All compounds with deshielded α-carbons (~100 ppm) and shielded β-carbons (~ 0 ppm) feature M−C$_\alpha$−C$_\beta$−C$_{\alpha'}$ torsional angles ξ close to 0°, short M−C$_{\alpha/\alpha'}$ and M···C$_\beta$ distances and elongated C$_{\alpha/\alpha'}$−C$_\beta$ bond distances and are active in metathesis. Inactive metallacyclobutanes have more shielded α-carbons (<50 ppm), more deshielded β-carbons (>20 ppm), and display normal M−C$_{\alpha/\alpha'}$ and C$_{\alpha/\alpha'}$−C$_\beta$ bond distances and long M···C$_\beta$ distances. In the metallacyclobutanes with deshielded α-carbons (~100 ppm) and torsion angles (ξ) close to 0°, the α_{ene} angle (between the H−C$_\alpha$−H plane and the M−C$_\alpha$ axis) is substantially larger (by 15−30°) than in those metallacyclobutanes with more shielded α-carbons and moving toward the values of alkylidene species (180°). The planarity of the M−C$_\alpha$−C$_\beta$−C$_{\alpha'}$ ring and the open α_{ene} angle indicates that C$_\alpha$ retains some alkylidene character since, for example, the α_{ene} angle in **Ti−Al−CB** is 154° and in **Ti-ene** is 180°. This correlation holds for the other metathesis-active metallacyclobutanes (Table S1).

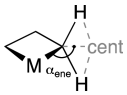

The main contribution to the paramagnetic deshielding on the α-carbons arises from the σ(M−C) bond. The associated coupled empty orbital corresponds to π^*(M−C), shown in red in Figure 2C, which develops into a full π^*(M═C) in an alkylidene (Figure 2D).[70,71,99−101] Consequently, the magnitude of the σ(M−C)/π^*(M−C) coupling increases when these orbitals are closer in energy, e.g., upon going from **Ti-CB** to **Ti-ene**, via **Ti−Al−CB**, **Ti-ene-PMe$_3$**, illustrating the remaining alkylidene character in metathesis-active metallacyclobutanes. While the α-carbon retains some of its alkylidene character upon metallacyclobutane formation, the β-carbon dramatically changes in comparison with its original olefinic character (Figure 3A,B), and becomes more shielded, reaching an isotropic chemical shift close to 0 ppm and changing the orientation of the shielding tensor at C$_\beta$. In contrast, the metallacyclobutanes that are inactive display shielding tensors similar to those of sp^3-carbons (Figure 3C).

The structures and electronic configurations that favor the occurrence of a low-lying empty orbital with π-character on the α-carbon in the plane of the metallacyclobutane perpendicular to the M−C$_\alpha$ direction are illustrated using **Ti-CB** as an example. The full qualitative MO diagram (in C_{2v} point group) is shown in Figure S12.[102,103] The relevant orbitals for this study are the occupied b_2 (blue) and a_1 (red) orbitals (Figure 4A). These orbitals with local M−C$_\alpha$ σ and π characters, are labeled {σ(M−C$_\alpha$) − σ(M−C$_{\alpha'}$)} and {π(M−C$_\alpha$) + π(M−C$_{\alpha'}$)}, respectively. The LUMO of a_1 symmetry (red) has local M−C$_\alpha$ π^* character ({π^*(M−C$_\alpha$) + π^*(M−C$_{\alpha'}$)} (Figure 4A).

The coupling of occupied {σ(M−C$_\alpha$) − σ(M−C$_{\alpha'}$)} and vacant {π^*(M−C$_\alpha$) + π^*(M−C$_{\alpha'}$)} through the angular momentum operator oriented perpendicularly to the ring ($\hat{L}_x$) represents the major contribution of what was described above in localized terms as the coupling of σ(M−C$_\alpha$) and π^*(M−C$_\alpha$). Thus, the magnitude of the coupling and hence the deshielding part of δ_{11} is qualitatively estimated by considering the coupling of these two orbitals, which depends on the difference in energy and the "overlap" between them (eq 4). The {σ(M−C$_\alpha$) − σ(M−C$_{\alpha'}$)} orbital has a large contribution on the carbons and can be considered to the first approximation as similar for all metallacyclobutanes. In contrast, {π^*(M−C$_\alpha$) + π^*(M−C$_{\alpha'}$)}, which is the LUMO for **Ti-CB** (Figure 4A), is mainly located on the metal center and is influenced by the ligand field and the electron configuration at the metal center. Thus, the magnitude of the paramagnetic term at the α-carbon can be assessed qualitatively by focusing on the characteristics (occupied vs empty, low vs high in energy, and spatial characteristics) of this orbital. These characteristics can be derived from the orbital splitting and electron occupations associated with the compounds.

For **Ti-CB** (and related d^0 **M-CB** complexes), the {π^*(M−C$_\alpha$) + π^*(M−C$_{\alpha'}$)} orbital, colored green in Figure 4B, is the LUMO, the metallacyclobutane is planar and the coupling is large, which leads to a large paramagnetic deshielding at the α-carbon (Figure 2). When this orbital is occupied as in **Mo-CB** [Cp$_2$Mo(CH$_2$CHRCH$_2$)] (red orbital in Figure 4C), no low-lying empty orbital is available and consequently the paramagnetic contribution is quenched; the α-carbons are shielded. In d^0 or d^4 L$_3$M(CH$_2$CH$_2$CH$_2$) complexes (**M-TBP**), the LUMO (green) has the same shape as in **Ti-CB**. It accounts for the large deshielding of the α-carbon in these complexes, whether they have d^0 or d^4 configurations as in **Mo-TBP**, **W-TBP** or **Ru-TBP** (Table S1). In the corresponding SP isomer, **M-SP**, there is also a low-lying empty orbital of similar shape (Figure 4C), but this orbital has poor "overlap" with the carbon backbone since the metal is out of the plane formed by the four equatorial ligands; it is thus represented in red. Consequently, the contribution of the paramagnetic term to δ_{11} originating from σ(M−C) is small and the α-carbon is not particularly deshielded. The d^6 octahedral complexes L$_4$M(CH$_2$CR$_2$CH$_2$) (**Ru-CB**, **Os-CB**, **Rh-CB**, **Ir-CB**, and **Pt-CB**) have no low-lying empty orbital on the metal, which results in shielded α-carbons. Accordingly, the α-carbons in these species retain no alkylidene character, and the metallacyclobutanes do not undergo [2 + 2]-cycloreversion and show no metathesis activity (Figure 4C). In **Ru-CB**, even upon loss of PMe$_3$, the chemical shift values of the metallacyclobutane barely change; the LUMO is oriented toward the empty coordination site and cannot contribute to deshielding of the α-carbon (Scheme S2). This contrasts with the **Ru-TBP** complex where large deshielding at the α-carbons is observed and calculated. In **Ru-TBP**, the metal LUMO (green orbital in Figure

DOI: 10.1021/acscentsci.7b00174
ACS Cent. Sci. 2017, 3, 759−768

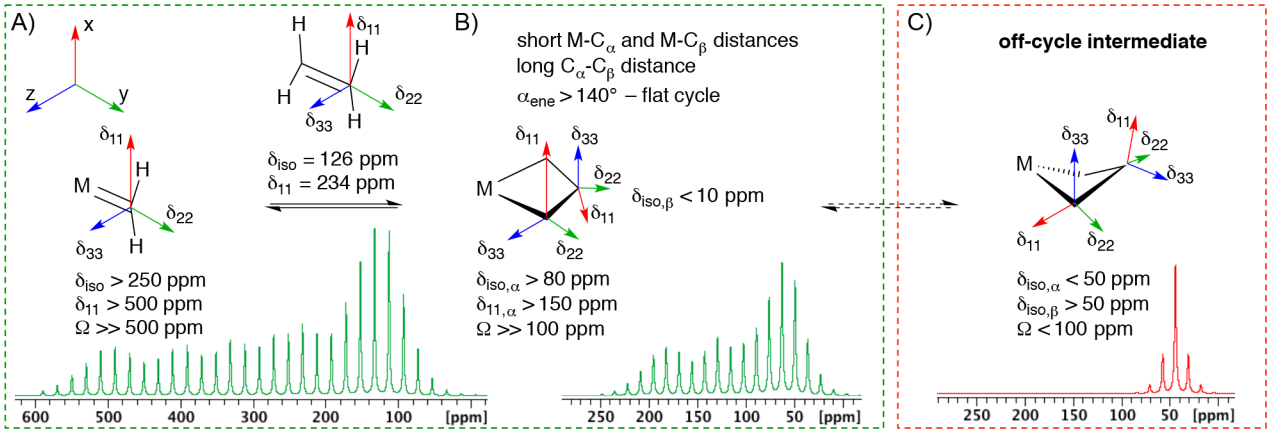

Figure 3. Orientation of the chemical shift tensors: in alkylidenes and ethylene (A), in active metallacyclobutanes (B), and in related inactive metallacyclobutanes **M-SP** (C); Figure S11 shows similar results for other inactive metallacyclobutanes. Simulated spectra at a spinning rate of 2 kHz of a W-alkylidene and α-carbons of **W-TBP** and **W-SP** are shown below the corresponding structures.

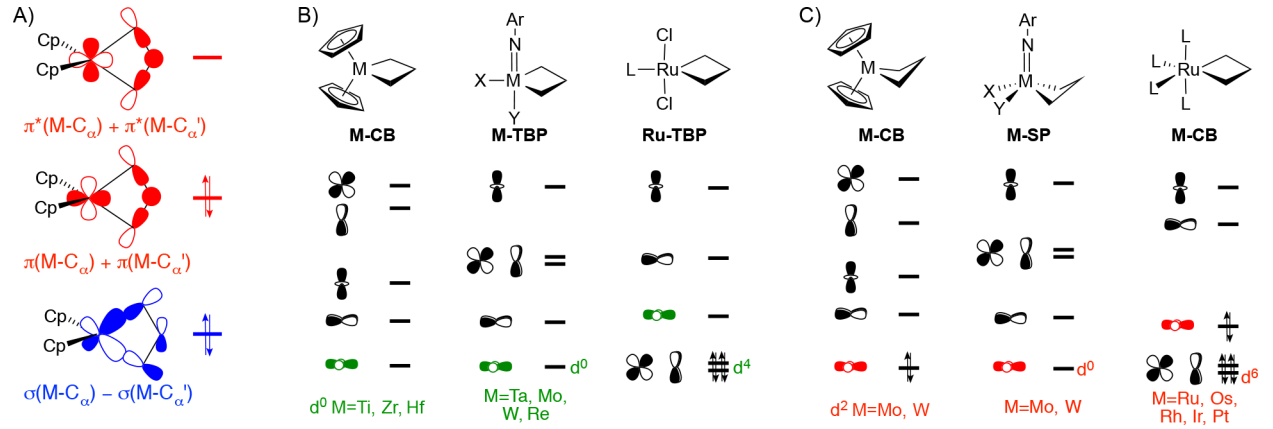

Figure 4. (A) Frontier orbitals of $Cp_2M(CH_2CH_2CH_2)$ determining the shielding (for full MO diagram and calculated plots of orbitals see Figure S12). Schematic d-orbital splitting for active (B) and inactive (C) metallacyclobutanes. The LUMO leading to the ^{13}C NMR chemical shifts characteristic of active metathesis catalysts is colored in green. The orbitals in red have the correct symmetry, but are either filled or not adequately directed to yield the characteristic ^{13}C NMR features of the active catalysts.

4B) is correctly positioned to induce a π-type overlap at the α-carbon. Consequently, **Ru-TBP** is a metallacyclobutane active in olefin metathesis whereas $(L_3)(PMe_3)Ru(CH_2CMe_2CH_2)$, an analogue of **Ru-CB**, has been shown to undergo β-methyl transfer[62] after loss of PMe_3 (Scheme S2). This analysis shows how the d-orbital splitting associated with the ligand field and the electron count determine the main contributions to the paramagnetic term of the carbon chemical shift tensor and the reactivity of the metallacyclobutane.

The shielded β-carbon of the **Ti-CB** and **M-TBP** metallacyclobutanes is associated with a planar ring ($\xi = 0°$) and with an open C_α–C_β–$C_{\alpha'}$ (110–120°) angle in comparison with the less shielded β-sp^3 carbon in **M-SP** metallacycles (e.g. $\xi = 27°$, C_α–C_β–$C_{\alpha'} = 97°$ in **W-SP**). The shielding of the β-carbon is due to a low paramagnetic contribution to σ_{11} and σ_{22} in combination with hardly any or even a slightly positive contribution to σ_{33} (Table S3), which is oriented perpendicularly to the plane of the metallacyclobutane in these compounds. This is best understood by analyzing the coupling between canonical orbitals: the orbital analysis of the paramagnetic term reveals that the *negative* contribution at the α-carbon and the *positive* contribution at the β-carbon, both in the direction perpendicular to the metallacyclobutane, are due to the coupling of the *same* occupied and empty canonical orbitals (Figure 4A and S12 for their calculated plots). This situation is similar to what is found for FCl, for which "paramagnetic contributions of opposite signs originate from the difference in relative phase of the p atomic orbitals at Cl and F in the highest occupied orbital" (Figure S13).[104] The presence of two p orbitals with opposite phases in the occupied MO leads to deshielding on the atom with dominant interaction, while the other atom is shielded. In the present case, the occupied orbital, described as $\{\sigma(M{-}C_\alpha) - \sigma(M{-}C_{\alpha'})\}$, has a similar change of phase between $M{-}C_{\alpha/\alpha'}$ and $C_{\alpha/\alpha'}{-}C_\beta$ (Figure S12C). Deshielding is obtained at $C_{\alpha/\alpha'}$ where the orbital interaction is larger while C_β is shielded (Figure S13).

It is informative to follow how the shielding tensors of the individual carbons change during the course of olefin metathesis, that is the reaction of the alkylidene and the olefin to yield the metallacyclobutane and the microscopic reverse (Figure 3A,B). The deshielding for σ_{11} on the α-carbon decreases upon metallacyclobutane formation, as the double bond of the alkylidene transforms into a metal–carbon single bond. However, the anisotropy remains large and the shielding tensor does not change its orientation illustrating the significant amount of alkylidene character preserved on the α-carbon in the active metallacyclobutane. A more dramatic change is observed for the β-carbon: upon metallacyclobutane formation the shielding tensor changes its orientation and magnitude, becoming much

DOI: 10.1021/acscentsci.7b00174
ACS Cent. Sci. 2017, 3, 759–768

less anisotropic and more shielded with now the most shielded component δ_{33} perpendicular to the ring (Figure 3B). While the α-carbons thus preserve their alkylidene character during the course of the reaction, it is quenched at the β-carbon. The change in orientation of the shielding tensor on the β-methylene carbon is similar to what is found on going from singlet CH_2[105] to CH_2^{2+} (Figure S14). In addition, the structure of metathesis-active metallacyclobutanes, with a wide $C_\alpha-C_\beta-C_{\alpha'}$ angle, is reminiscent of the σ-bond metathesis transition state (M−X + H−X), which is associated with a wide $X_\alpha-H_\beta-X_{\alpha'}$ angle (X = H or CH_2R).[106,107] At this transition state, the β-H is migrating as a proton between two anionic X ligands. Analogously, in active metallacyclobutanes, the β-CH_2 group can thus be viewed as a migrating four-electron fragment — with two empty orbitals at carbon — between two eight-electron methylenes. As two σ bonds are broken and formed during σ-bond metathesis, two σ and two π bonds are involved during olefin metathesis.

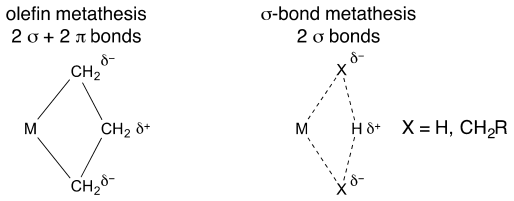

In fact, CH_2^{2+} is isolobal with Cp_2Ti^{2+},[103,108] making $Cp_2Ti(CH_2CH_2CH_2)$ isolobal with $Cp_2Ti(\mu^2\text{-}CH_2)_2TiCp_2$. This known compound[109,110] displays a shielding tensor for the α-carbon with the same orientation (Figure S15) and a δ_{iso} for the bridging methylene (observed value of 236 ppm) intermediate between the values calculated for the alkylidene **Ti-ene** (338 ppm) and the α-CH_2 in **Ti-CB** (81 ppm), further supporting that the β-carbon is transferred as a formal CH_2^{2+} fragment with the α-carbon retaining the alkylidene character modulated by the metal center.

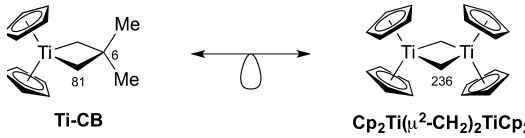

In all metathesis-active metallacyclobutanes, such as **Ti-CB** and **M-TBP**, the rearrangement of both the π- and the σ-framework is evidenced by a long $C_\alpha-C_\beta$ bond (>1.56 Å) and the change of orientation of the shielding tensor on the β-carbon, as a formally four-electron CR_2 fragment is transferred between two alkylidene-like α-carbons. In the corresponding **M-SP**, observed with some Schrock type metathesis catalysts,[16,29] the orientation of the shielding tensor and the magnitude of the principal components of the α- and β-carbons are typical of sp^3-carbons (Figure 3C); the α-carbon has lost its alkylidene character and the metal−carbon and carbon−carbon bonds are regular σ-bonds. Therefore, **M-SP** is not a reactive intermediate in olefin metathesis. It is an off-cycle resting state that needs to isomerize to **M-TBP** to re-enter the catalytic cycle.[11−16]

CONCLUSIONS

The principal components of the ^{13}C chemical shift tensors in metallacyclobutanes and related structures, in particular σ_{11}/δ_{11}, provide important information about the electronic structure in general and the frontier orbitals in particular of these compounds. The experimental and computational studies allow a relation between isotropic chemical shift values and olefin metathesis reactivity to be developed. In particular, the metallacyclobutanes with chemical shift for the α- and β-carbons of ca. 100−80 and 0 ppm, respectively, are active in metathesis and directly involved in the metathesis pathway, while those with isotropic chemical shifts of less than 50 ppm for the α-carbon and more than 20 ppm for the β-carbon are inactive. The high ^{13}C chemical shifts on the α-carbon in metathesis active metallacyclobutanes are a consequence of the presence of a low-lying empty orbital with alkylidene character (π^*) on this carbon. This orbital is present in d^0 and d^4 pentacoordinated TBP and in d^0 Cp_2M metallacyclobutanes. This character can only develop in a planar metallacyclobutane. A consequence of this geometry is that the saturated CR_2 fragment, which transfers into and out of the metallacyclobutane, is shielded perpendicularly to the ring. In the absence of a low-lying empty orbital such as in d^0 **M-SP**, d^2 **Mo-CB**, or d^6 octahedral complexes, the metallacyclobutane cannot participate in the metathesis reaction. Measuring and analyzing the principal components of the chemical shift tensor provide invaluable information on the topology and energy of the molecular orbitals and mechanistic insight into the olefin metathesis reaction and perhaps other reactions of importance in organometallic chemistry. We are currently exploring this field of research.

ASSOCIATED CONTENT

Supporting Information

The Supporting Information is available free of charge on the ACS Publications website at DOI: 10.1021/acscentsci.7b00174.

Experimental and computational details, NCS analysis, graphical representations of all calculated shielding tensors, molecular orbital diagram of $Cp_2TiCH_2CR_2CH_2$ and plot of molecular orbitals, experimental solid-state NMR spectra, X-ray structure of **Ru-CB**, coordinates of all presented species (PDF)

AUTHOR INFORMATION

Corresponding Authors

*E-mail: raandersen@lbl.gov (R.A.A.).
*E-mail: ccoperet@ethz.ch (C.C.).
*E-mail: christophe.raynaud1@umontpellier.fr (C.R.).
*E-mail: odile.eisenstein@univ-montp2.fr (O.E.).

ORCID

Christopher P. Gordon: 0000-0002-2199-8995
Keishi Yamamoto: 0000-0001-5241-078X
Wei-Chih Liao: 0000-0002-4656-6291
Christophe Copéret: 0000-0001-9660-3890
Christophe Raynaud: 0000-0003-0979-2051
Odile Eisenstein: 0000-0001-5056-0311

Author Contributions

#C.P.G. and K.Y. contributed equally. The syntheses of all compounds were carried out by K.Y., C.P.G., and F.A. The NMR measurements were done by W.C.L., computations were performed by C.P.G. and C.R. Interpretation of NCS analysis was carried out by C.P.G., C.C., R.A.A., C.R., and O.E. All authors participated in the writing of the manuscript.

Notes

The authors declare no competing financial interest.

ACKNOWLEDGMENTS

Dr. T.-C. Ong is acknowledged for preliminary NMR measurements on a related compound to **Ti-CB**. K.Y. thanks the Canon

DOI: 10.1021/acscentsci.7b00174
ACS Cent. Sci. 2017, 3, 759−768

foundation for a postdoctoral fellowship. The work of C.P.G. and W.C.L. is supported by SNF Grant Number 200021_169134 and 200020_149704, respectively. The computations were performed using HPC resources of CINES and IDRIS under the allocation 2016-087529. C.R. and O.E. thank the CNRS and the Université de Montpellier for funding. O.E. was supported by the Research Council of Norway (RCN) through the CoE Centre for Theoretical and Computational Chemistry (CTCC) Grant No. 179568/V30 and 171185/V30. C.C. and O.E. thank the Miller fellowship program of UC Berkeley, where discussions with R.A.A. started.

REFERENCES

(1) Grubbs, R. H.; Chang, S. Recent Advances in Olefin Metathesis and its Application in Organic Synthesis. *Tetrahedron* **1998**, *54*, 4413−4450.
(2) Fürstner, A. Olefin Metathesis and Beyond. *Angew. Chem., Int. Ed.* **2000**, *39*, 3012−3043.
(3) Schrock, R. R. High Oxidation State Multiple Metal−Carbon Bonds. *Chem. Rev.* **2002**, *102*, 145−180.
(4) Hoveyda, A. H.; Zhugralin, A. R. The Remarkable Metal-Catalysed Olefin Metathesis Reaction. *Nature* **2007**, *450*, 243−251.
(5) Fürstner, A. Metathesis in Total Synthesis. *Chem. Commun.* **2011**, *47*, 6505−6511.
(6) Grela, K. *Olefin Metathesis: Theory and Practice*; Wiley VCH: Weinheim, 2014.
(7) Grubbs, R. H.; Wenzel, A. G.; O'Leary, D. J.; Khosravi, E. *Handbook of Metathesis, 3 Vol. Set*, 2nd ed.; Wiley VCH: Weinheim, 2015.
(8) Higman, C. S.; Lummiss, J. A. M.; Fogg, D. E. Olefin Metathesis at the Dawn of Implementation in Pharmaceutical and Specialty-Chemicals Manufacturing. *Angew. Chem., Int. Ed.* **2016**, *55*, 3552−3565.
(9) Hérisson, P. J.-L.; Chauvin, Y. Catalyse de Transformation des Oléfines par les Complexes Du Tungstène. II. Télomérisation des Oléfines Cycliques en Présence d'Oléfines Acycliques. *Makromol. Chem.* **1971**, *141*, 161−176.
(10) Chauvin, Y. Olefin Metathesis: The Early Days (Nobel Lecture). *Angew. Chem., Int. Ed.* **2006**, *45*, 3740−3747.
(11) Solans-Monfort, X.; Clot, E.; Copéret, C.; Eisenstein, O. d^0 Re-Based Olefin Metathesis Catalysts, Re(≡CR)(═CHR)(X)(Y): The Key Role of X and Y Ligands for Efficient Active Sites. *J. Am. Chem. Soc.* **2005**, *127*, 14015−14025.
(12) Poater, A.; Solans-Monfort, X.; Clot, E.; Copéret, C.; Eisenstein, O. Understanding d^0-Olefin Metathesis Catalysts: Which Metal, Which Ligands? *J. Am. Chem. Soc.* **2007**, *129*, 8207−8216.
(13) Leduc, A.-M.; Salameh, A.; Soulivong, D.; Chabanas, M.; Basset, J.-M.; Copéret, C.; Solans-Monfort, X.; Clot, E.; Eisenstein, O.; Böhm, V. P. W.; Röper, M. β-H Transfer from the Metallacyclobutane: A Key Step in the Deactivation and Byproduct Formation for the Well-Defined Silica-Supported Rhenium Alkylidene Alkene Metathesis Catalyst. *J. Am. Chem. Soc.* **2008**, *130*, 6288−6297.
(14) Solans-Monfort, X.; Copéret, C.; Eisenstein, O. Shutting Down Secondary Reaction Pathways: The Essential Role of the Pyrrolyl Ligand in Improving Silica Supported d^0-ML_4 Alkene Metathesis Catalysts from DFT Calculations. *J. Am. Chem. Soc.* **2010**, *132*, 7750−7757.
(15) Solans-Monfort, X.; Copéret, C.; Eisenstein, O. Oxo vs Imido Alkylidene d^0-Metal Species: How and why do they Differ in Structure, Activity, and Efficiency in Alkene Metathesis? *Organometallics* **2012**, *31*, 6812−6822.
(16) Solans-Monfort, X.; Copéret, C.; Eisenstein, O. Metallacyclobutanes from Schrock-Type d^0 Metal Alkylidene Catalysts: Structural Preferences and Consequences in Alkene Metathesis. *Organometallics* **2015**, *34*, 1668−1680.
(17) Feldman, J.; Schrock, R. R., Recent Advances in the Chemistry of "d^0" Alkylidene and Metallacyclobutane Complexes. In *Prog. Inorg. Chem.*; John Wiley & Sons, Inc., 1991; pp 1−74.
(18) Schrock, R. R.; Hoveyda, A. H. Molybdenum and Tungsten Imido Alkylidene Complexes as Efficient Olefin-Metathesis Catalysts. *Angew. Chem., Int. Ed.* **2003**, *42*, 4592−4633.
(19) Schrock, R. R. Multiple Metal−Carbon Bonds for Catalytic Metathesis Reactions (Nobel Lecture). *Angew. Chem., Int. Ed.* **2006**, *45*, 3748−3759.
(20) Schrock, R. R. Recent Advances in High Oxidation State Mo and W Imido Alkylidene Chemistry. *Chem. Rev.* **2009**, *109*, 3211−3226.
(21) Wallace, K. C.; Dewan, J. C.; Schrock, R. R. Multiple Metal-Carbon Bonds. 44. Isolation and Characterization of the First Simple Tantalacyclobutane Complexes. *Organometallics* **1986**, *5*, 2162−2164.
(22) Wallace, K. C.; Liu, A. H.; Dewan, J. C.; Schrock, R. R. Preparation and Reactions of Tantalum Alkylidene Complexes Containing Bulky Phenoxide or Thiolate Ligands. Controlling Ring-Opening Metathesis Polymerization Activity and Mechanism through Choice of Anionic Ligand. *J. Am. Chem. Soc.* **1988**, *110*, 4964−4977.
(23) Feldman, J.; Murdzek, J. S.; Davis, W. M.; Schrock, R. R. Reaction of Neopentylidene Complexes of the Type M(CH-t-Bu)(N-2,6-C_6H_3-i-Pr_2) $(OR)_2$ (M = W, Mo) with Methyl Acrylate and N,N-Dimethylacrylamide to Give Metallacyclobutane Complexes. *Organometallics* **1989**, *8*, 2260−2265.
(24) Marinescu, S. C.; Schrock, R. R.; Müller, P.; Hoveyda, A. H. Ethenolysis Reactions Catalyzed by Imido Alkylidene Monoaryloxide Monopyrrolide (MAP) Complexes of Molybdenum. *J. Am. Chem. Soc.* **2009**, *131*, 10840−10841.
(25) Liu, A. H.; Murray, R. C.; Dewan, J. C.; Santarsiero, B. D.; Schrock, R. R. High Oxidation State Monopentamethylcyclopentadienyltungsten Methyl Complexes Including the First d^0 Complex Containing a Highly Distorted Methylene Ligand, W(η^5-C_5Me_5)$(CH_3)_3(CH_2)$. *J. Am. Chem. Soc.* **1987**, *109*, 4282−4291.
(26) Schrock, R. R.; DePue, R. T.; Feldman, J.; Schaverien, C. J.; Dewan, J. C.; Liu, A. H. Preparation and Reactivity of Several Alkylidene Complexes of the Type W(CHR′)(N-2,6-C_6H_3-i-Pr_2) $(OR)_2$ and Related Tungstacyclobutane Complexes. Controlling Metathesis Activity through the Choice of Alkoxide Ligand. *J. Am. Chem. Soc.* **1988**, *110*, 1423−1435.
(27) Feldman, J.; Davis, W. M.; Schrock, R. R. Trigonal-Bipyramidal and Square-Pyramidal Tungstacyclobutane Intermediates are Both Present in Systems in Which Olefins are Metathesized by Complexes of the Type W(CHR′)(N-2,6-C_6H_3-i-Pr_2) $(OR)_2$. *Organometallics* **1989**, *8*, 2266−2268.
(28) Schrock, R. R.; DePue, R. T.; Feldman, J.; Yap, K. B.; Yang, D. C.; Davis, W. M.; Park, L.; DiMare, M.; Schofield, M. Further Studies of Imido Alkylidene Complexes of Tungsten, Well-Characterized Olefin Metathesis Catalysts with Controllable Activity. *Organometallics* **1990**, *9*, 2262−2275.
(29) Feldman, J.; Davis, W. M.; Thomas, J. K.; Schrock, R. R. Preparation and Reactivity of Tungsten(VI) Metallacyclobutane Complexes. Square Pyramids Versus Trigonal Bipyramids. *Organometallics* **1990**, *9*, 2535−2548.
(30) Vaughan, G. A.; Toreki, R.; Schrock, R. R.; Davis, W. M. Reversible "3 + 2 Cycloaddition" of Ethylene to the C═Re≡C Unit in Rhenium Complexes of the Type Re(C-*t*-Bu) (CHR′) $(OR)_2$. *J. Am. Chem. Soc.* **1993**, *115*, 2980−2981.
(31) Copéret, C.; Chabanas, M.; Petroff Saint-Arroman, R.; Basset, J.-M. Homogeneous and Heterogeneous Catalysis: Bridging the Gap through Surface Organometallic Chemistry. *Angew. Chem., Int. Ed.* **2003**, *42*, 156−181.
(32) Copéret, C. Design and Understanding of Heterogeneous Alkene Metathesis Catalysts. *Dalton Trans.* **2007**, 5498−5504.
(33) Copéret, C.; Comas-Vives, A.; Conley, M. P.; Estes, D. P.; Fedorov, A.; Mougel, V.; Nagae, H.; Núñez-Zarur, F.; Zhizhko, P. A. Surface Organometallic and Coordination Chemistry toward Single-Site Heterogeneous Catalysts: Strategies, Methods, Structures, and Activities. *Chem. Rev.* **2016**, *116*, 323−421.
(34) Blanc, F.; Berthoud, R.; Copéret, C.; Lesage, A.; Emsley, L.; Singh, R.; Kreickmann, T.; Schrock, R. R. Direct Observation of Reaction Intermediates for a Well Defined Heterogeneous Alkene Metathesis Catalyst. *Proc. Natl. Acad. Sci. U. S. A.* **2008**, *105*, 12123−12127.
(35) Mougel, V.; Copéret, C. Magnitude and Consequences of Ligand σ-Donation on Alkene Metathesis Activity in d^0 Silica Supported (≡

DOI: 10.1021/acscentsci.7b00174
ACS Cent. Sci. 2017, 3, 759−768

SiO)W(NAr)(=CHtBu) (OR) Catalysts. *Chem. Sci.* **2014**, *5*, 2475−2481.
(36) Conley, M. P.; Forrest, W. P.; Mougel, V.; Copéret, C.; Schrock, R. R. Bulky Aryloxide Ligand Stabilizes a Heterogeneous Metathesis Catalyst. *Angew. Chem., Int. Ed.* **2014**, *53*, 14221−14224.
(37) Mougel, V.; Santiago, C. B.; Zhizhko, P. A.; Bess, E. N.; Varga, J.; Frater, G.; Sigman, M. S.; Copéret, C. Quantitatively Analyzing Metathesis Catalyst Activity and Structural Features in Silica-Supported Tungsten Imido−Alkylidene Complexes. *J. Am. Chem. Soc.* **2015**, *137*, 6699−6704.
(38) Mougel, V.; Chan, K.-W.; Siddiqi, G.; Kawakita, K.; Nagae, H.; Tsurugi, H.; Mashima, K.; Safonova, O.; Copéret, C. Low Temperature Activation of Supported Metathesis Catalysts by Organosilicon Reducing Agents. *ACS Cent. Sci.* **2016**, *2*, 569−576.
(39) Ong, T.-C.; Liao, W.-C.; Mougel, V.; Gajan, D.; Lesage, A.; Emsley, L.; Copéret, C. Atomistic Description of Reaction Intermediates for Supported Metathesis Catalysts Enabled by DNP SENS. *Angew. Chem., Int. Ed.* **2016**, *55*, 4743−4747.
(40) Mougel, V.; Pucino, M.; Copéret, C. Strongly σ Donating Thiophenoxide in Silica-Supported Tungsten Oxo Catalysts for Improved 1-Alkene Metathesis Efficiency. *Organometallics* **2015**, *34*, 551−554.
(41) Allouche, F.; Mougel, V.; Copéret, C. Activating Thiolate-Based Imidoalkylidene Tungsten(VI) Metathesis Catalysts by Grafting onto Silica. *Asian J. Org. Chem.* **2015**, *4*, 528−532.
(42) Valla, M.; Wischert, R.; Comas-Vives, A.; Conley, M. P.; Verel, R.; Copéret, C.; Sautet, P. Role of Tricoordinate Al Sites in CH_3ReO_3/Al_2O_3 Olefin Metathesis Catalysts. *J. Am. Chem. Soc.* **2016**, *138*, 6774−6785.
(43) Romero, P. E.; Piers, W. E. Direct Observation of a 14-Electron Ruthenacyclobutane Relevant to Olefin Metathesis. *J. Am. Chem. Soc.* **2005**, *127*, 5032−5033.
(44) Wenzel, A. G.; Grubbs, R. H. Ruthenium Metallacycles Derived from 14-Electron Complexes. New Insights into Olefin Metathesis Intermediates. *J. Am. Chem. Soc.* **2006**, *128*, 16048−16049.
(45) van der Eide, E. F.; Romero, P. E.; Piers, W. E. Generation and Spectroscopic Characterization of Ruthenacyclobutane and Ruthenium Olefin Carbene Intermediates Relevant to Ring Closing Metathesis Catalysis. *J. Am. Chem. Soc.* **2008**, *130*, 4485−4491.
(46) Cavallo, L. Mechanism of Ruthenium-Catalyzed Olefin Metathesis Reactions from a Theoretical Perspective. *J. Am. Chem. Soc.* **2002**, *124*, 8965−8973.
(47) Adlhart, C.; Chen, P. Mechanism and Activity of Ruthenium Olefin Metathesis Catalysts: The Role of Ligands and Substrates from a Theoretical Perspective. *J. Am. Chem. Soc.* **2004**, *126*, 3496−3510.
(48) Occhipinti, G.; Bjørsvik, H.-R.; Jensen, V. R. Quantitative Structure−Activity Relationships of Ruthenium Catalysts for Olefin Metathesis. *J. Am. Chem. Soc.* **2006**, *128*, 6952−6964.
(49) Webster, C. E. Computational Insights into Degenerate Ethylene Exchange with a Grubbs-Type Catalyst. *J. Am. Chem. Soc.* **2007**, *129*, 7490−7491.
(50) Poater, A.; Ragone, F.; Correa, A.; Szadkowska, A.; Barbasiewicz, M.; Grela, K.; Cavallo, L. Mechanistic Insights into the Cis−Trans Isomerization of Ruthenium Complexes Relevant to Catalysis of Olefin Metathesis. *Chem. - Eur. J.* **2010**, *16*, 14354−14364.
(51) Tebbe, F. N.; Parshall, G. W.; Reddy, G. S. Olefin Homologation with Titanium Methylene Compounds. *J. Am. Chem. Soc.* **1978**, *100*, 3611−3613.
(52) Howard, T. R.; Lee, J. B.; Grubbs, R. H. Titanium Metallacarbene-Metallacyclobutane Reactions: Stepwise Metathesis. *J. Am. Chem. Soc.* **1980**, *102*, 6876−6878.
(53) Eisenstein, O.; Hoffmann, R.; Rossi, A. R. Some Geometrical and Electronic Features of the Intermediate Stages of Olefin Metathesis. *J. Am. Chem. Soc.* **1981**, *103*, 5582−5584.
(54) Dedieu, A.; Eisenstein, O. Metallacyclobutanes: Are They Distorted? A Theoretical Ab-Inito Study. *Nouv. J. Chim.* **1982**, *6*, 337−340.
(55) Gilliom, L. R.; Grubbs, R. H. Titanacyclobutanes Derived from Strained, Cyclic Olefins: The Living Polymerization of Norbornene. *J. Am. Chem. Soc.* **1986**, *108*, 733−742.
(56) Straus, D. A.; Grubbs, R. H. Titanacyclobutanes: Substitution Pattern and Stability. *Organometallics* **1982**, *1*, 1658−1661.
(57) Scheins, S.; Messerschmidt, M.; Gembicky, M.; Pitak, M.; Volkov, A.; Coppens, P.; Harvey, B. G.; Turpin, G. C.; Arif, A. M.; Ernst, R. D. Charge Density Analysis of the (C−C)→Ti Agostic Interactions in a Titanacyclobutane Complex. *J. Am. Chem. Soc.* **2009**, *131*, 6154−6160.
(58) Seetz, J. W. F. L.; Schat, G.; Akkerman, O. S.; Bickelhaupt, F. Zircona- and Hafnacyclobutenes—a New Route to Metallacyclobutanes. *Angew. Chem., Int. Ed. Engl.* **1983**, *22*, 248−249.
(59) Ephritikhine, M.; Francis, B. R.; Green, M. L. H.; Mackenzie, R. E.; Smith, M. J. Bis(η-Cyclopentadienyl)-Molybdenum and -Tungsten Chemistry: σ- and η-Allylic and Metallacyclobutane Derivatives. *J. Chem. Soc., Dalton Trans.* **1977**, 1131−1135.
(60) Harvey, B. G.; Mayne, C. L.; Arif, A. M.; Ernst, R. D. Structural and Spectroscopic Demonstration of Agostic C−C Interactions in Electron-Deficient Metallacyclobutanes and Related Cage Complexes: Possible Implications for Olefin Polymerizations and Metatheses. *J. Am. Chem. Soc.* **2005**, *127*, 16426−16435.
(61) Andersen, R. A.; Jones, R. A.; Wilkinson, G. Trimethylsilylmethyl and Other Alkyls of Chromium, Molybdenum, Ruthenium, and Rhodium from Interaction of Magnesium Dialkyls with Metal-Metal Bonded Binuclear Acetates of Chromium(II), Molybdenum(II), Ruthenium(II, III), and Rhodium(II). *J. Chem. Soc., Dalton Trans.* **1978**, 446−453.
(62) McNeill, K.; Andersen, R. A.; Bergman, R. G. C−C and C−H Bond Activation at Ruthenium(II): The Stepwise Degradation of a Neopentyl Ligand to a Trimethylenemethane Ligand. *J. Am. Chem. Soc.* **1997**, *119*, 11244−11254.
(63) Lindner, E.; Jansen, R.-M.; Hiller, W.; Fawzi, R. Darstellung und Eigenschaften von und Reaktionen mit Metallhaltigen Heterocyclen, LXIV: Darstellung und Untersuchungen zur Reaktivität von H_2-Olefin-Komplexen Und Vier- bis Sechsgliedrigen Metallacycloalkanen Von Ruthenium und Osmium. *Chem. Ber.* **1989**, *122*, 1403−1409.
(64) Diversi, P.; Inogrosso, G.; Luherini, A.; Fasce, D. C(sp^3)-H and C(sp^2)-H Bond Activation in the (Pentamethylcyclo-pentadienyl)-rhodium(III) System: Formation of (2,2-Dimethylpropane-1,3-diyl)(pentamethylcyclopentadienyl) (triphenylphosphine)rhodium and Neopentyl(pentamethylcyclopentadienyl) (triphenylphosphine-C^2,P)-rhodium. *J. Chem. Soc., Chem. Commun.* **1982**, 945−946.
(65) Tulip, T. H.; Thorn, D. L. Hydridometallacycloalkane Complexes of Iridium. Unassisted Intramolecular Distal Carbon-Hydrogen Bond Activation. *J. Am. Chem. Soc.* **1981**, *103*, 2448−2450.
(66) Adams, D. M.; Chatt, J.; Guy, R. G.; Sheppard, N. The Structure of "Cyclopropane Platinous Chloride". *J. Chem. Soc.* **1961**, *0*, 738−742.
(67) Puddephatt, R. J. Platinacyclobutane Chemistry. *Coord. Chem. Rev.* **1980**, *33*, 149−194.
(68) Jennings, P. W.; Johnson, L. L. Metallacyclobutane Complexes of the Group Eight Transition Metals: Synthesis, Characterizations, and Chemistry. *Chem. Rev.* **1994**, *94*, 2241−2290.
(69) Widdifield, C. M.; Schurko, R. W. Understanding Chemical Shielding Tensors Using Group Theory, MO Analysis, and Modern Density-Functional Theory. *Concepts Magn. Reson., Part A* **2009**, *34A*, 91−123.
(70) Halbert, S.; Copéret, C.; Raynaud, C.; Eisenstein, O. Elucidating the Link between NMR Chemical Shifts and Electronic Structure in d^0 Olefin Metathesis Catalysts. *J. Am. Chem. Soc.* **2016**, *138*, 2261−2272.
(71) Yamamoto, K.; Gordon, C. P.; Liao, W.-C.; Copéret, C.; Raynaud, C.; Eisenstein, O. Orbital Analysis of Carbon-13 Chemical Shift Tensors Reveals Patterns to Distinguish Fischer and Schrock Carbenes. *Angew. Chem., Int. Ed.* **2017**, DOI: 10.1002/anie.201701537
(72) Herzfeld, J.; Berger, A. E. Sideband Intensities in NMR Spectra of Samples Spinning at the Magic Angle. *J. Chem. Phys.* **1980**, *73*, 6021−6030.
(73) Bohmann, J. A.; Weinhold, F.; Farrar, T. C. Natural Chemical Shielding Analysis of Nuclear Magnetic Resonance Shielding Tensors

DOI: 10.1021/acscentsci.7b00174
ACS Cent. Sci. 2017, 3, 759−768

from Gauge-Including Atomic Orbital Calculations. *J. Chem. Phys.* **1997**, *107*, 1173−1184.
(74) Autschbach, J. Analyzing NMR Shielding Tensors Calculated with Two-Component Relativistic Methods Using Spin-Free Localized Molecular Orbitals. *J. Chem. Phys.* **2008**, *128*, 164112.
(75) Autschbach, J.; Zheng, S. Analyzing Pt Chemical Shifts Calculated from Relativistic Density Functional Theory Using Localized Orbitals: The Role of Pt 5d Lone Pairs. *Magn. Reson. Chem.* **2008**, *46*, S45−S55.
(76) Aquino, F.; Pritchard, B.; Autschbach, J. Scalar Relativistic Computations and Localized Orbital Analyses of Nuclear Hyperfine Coupling and Paramagnetic NMR Chemical Shifts. *J. Chem. Theory Comput.* **2012**, *8*, 598−609.
(77) Ruiz-Morales, Y.; Schreckenbach, G.; Ziegler, T. Origin of the Hydridic ^{1}H NMR Chemical Shift in Low-Valent Transition-Metal Hydrides. *Organometallics* **1996**, *15*, 3920−3923.
(78) Wu, G.; Rovnyak, D.; Johnson, M. J. A.; Zanetti, N. C.; Musaev, D. G.; Morokuma, K.; Schrock, R. R.; Griffin, R. G.; Cummins, C. C. Unusual ^{31}P Chemical Shielding Tensors in Terminal Phosphido Complexes Containing a Phosphorus−Metal Triple Bond. *J. Am. Chem. Soc.* **1996**, *118*, 10654−10655.
(79) Ruiz-Morales, Y.; Schreckenbach, G.; Ziegler, T. Theoretical Study of ^{13}C and ^{17}O NMR Shielding Tensors in Transition Metal Carbonyls Based on Density Functional Theory and Gauge-Including Atomic Orbitals. *J. Phys. Chem.* **1996**, *100*, 3359−3367.
(80) Wiberg, K. B.; Hammer, J. D.; Zilm, K. W.; Cheeseman, J. R. NMR Chemical Shifts. 3. A Comparison of Acetylene, Allene, and the Higher Cumulenes. *J. Org. Chem.* **1999**, *64*, 6394−6400.
(81) Auer, D.; Strohmann, C.; Arbuznikov, A. V.; Kaupp, M. Understanding Substituent Effects on ^{29}Si Chemical Shifts and Bonding in Disilenes. A Quantum Chemical Analysis. *Organometallics* **2003**, *22*, 2442−2449.
(82) Auer, D.; Kaupp, M.; Strohmann, C. Unexpected" ^{29}Si NMR Chemical Shifts in Heteroatom-Substituted Silyllithium Compounds: A Quantum-Chemical Analysis. *Organometallics* **2004**, *23*, 3647−3655.
(83) Sceats, E. L.; Figueroa, J. S.; Cummins, C. C.; Loening, N. M.; Van der Wel, P.; Griffin, R. G. Complexes Obtained by Electrophilic Attack on a Dinitrogen-Derived Terminal Molybdenum Nitride: Electronic Structure Analysis by Solid State CP/MAS ^{15}N NMR in Combination with DFT Calculations. *Polyhedron* **2004**, *23*, 2751−2768.
(84) Karni, M.; Apeloig, Y.; Takagi, N.; Nagase, S. Ab Initio and DFT Study of the ^{29}Si NMR Chemical Shifts in RSi≡SiR. *Organometallics* **2005**, *24*, 6319−6330.
(85) Kravchenko, V.; Kinjo, R.; Sekiguchi, A.; Ichinohe, M.; West, R.; Balazs, Y. S.; Schmidt, A.; Karni, M.; Apeloig, Y. Solid-State ^{29}Si NMR Study of RSiSiR: A Tool for Analyzing the Nature of the Si−Si Bond. *J. Am. Chem. Soc.* **2006**, *128*, 14472−14473.
(86) Rossini, A. J.; Mills, R. W.; Briscoe, G. A.; Norton, E. L.; Geier, S. J.; Hung, I.; Zheng, S.; Autschbach, J.; Schurko, R. W. Solid-State Chlorine NMR of Group IV Transition Metal Organometallic Complexes. *J. Am. Chem. Soc.* **2009**, *131*, 3317−3330.
(87) Epping, J. D.; Yao, S.; Karni, M.; Apeloig, Y.; Driess, M. Si═X Multiple Bonding with Four-Coordinate Silicon? Insights into the Nature of the Si═O and Si═S Double Bonds in Stable Silanoic Esters and Related Thioesters: A Combined NMR Spectroscopic and Computational Study. *J. Am. Chem. Soc.* **2010**, *132*, 5443−5455.
(88) Standara, S.; Bouzkova, K.; Straka, M.; Zacharova, Z.; Hocek, M.; Marek, J.; Marek, R. Interpretation of Substituent Effects on ^{13}C and ^{15}N NMR Chemical Shifts in 6-Substituted Purines. *Phys. Chem. Chem. Phys.* **2011**, *13*, 15854−15864.
(89) Zhu, J.; Kurahashi, T.; Fujii, H.; Wu, G. Solid-State ^{17}O NMR and Computational Studies of Terminal Transition Metal Oxo Compounds. *Chem. Sci.* **2012**, *3*, 391−397.
(90) Toušek, J.; Straka, M.; Sklenář, V.; Marek, R. Origin of the Conformational Modulation of the ^{13}C NMR Chemical Shift of Methoxy Groups in Aromatic Natural Compounds. *J. Phys. Chem. A* **2013**, *117*, 661−669.
(91) Pascual-Borras, M.; Lopez, X.; Rodriguez-Fortea, A.; Errington, R. J.; Poblet, J. M. ^{17}O NMR Chemical Shifts in Oxometalates: From the Simplest Monometallic Species to Mixed-Metal Polyoxometalates. *Chem. Sci.* **2014**, *5*, 2031−2042.
(92) Vícha, J.; Straka, M.; Munzarová, M. L.; Marek, R. Mechanism of Spin−Orbit Effects on the Ligand NMR Chemical Shift in Transition-Metal Complexes: Linking NMR to EPR. *J. Chem. Theory Comput.* **2014**, *10*, 1489−1499.
(93) Pascual-Borras, M.; Lopez, X.; Poblet, J. M. Accurate Calculation of ^{31}P NMR Chemical Shifts in Polyoxometalates. *Phys. Chem. Chem. Phys.* **2015**, *17*, 8723−8731.
(94) Vummaleti, S. V. C.; Nelson, D. J.; Poater, A.; Gomez-Suarez, A.; Cordes, D. B.; Slawin, A. M. Z.; Nolan, S. P.; Cavallo, L. What Can NMR Spectroscopy of Selenoureas and Phosphinidenes Teach Us About the π-Accepting Abilities of N-Heterocyclic Carbenes? *Chem. Sci.* **2015**, *6*, 1895−1904.
(95) Lummiss, J. A. M.; Perras, F. A.; McDonald, R.; Bryce, D. L.; Fogg, D. E. Sterically Driven Olefin Metathesis: The Impact of Alkylidene Substitution on Catalyst Activity. *Organometallics* **2016**, *35*, 691−698.
(96) Haller, L. J. L.; Mas-Marza, E.; Cybulski, M. K.; Sanguramath, R. A.; Macgregor, S. A.; Mahon, M. F.; Raynaud, C.; Russell, C. A.; Whittlesey, M. K. Computation Provides Chemical Insight into the Diverse Hydride NMR Chemical Shifts of $[Ru(NHC)_4(L)H]^{0/+}$ Species (NHC = N-Heterocyclic Carbene; L = Vacant, H_2, N_2, CO, MeCN, O_2, P_4, SO_2, H^-, F^- and Cl^-) and Their $[Ru(R_2PCH_2CH_2PR_2)_2(L)H]^+$ Congeners. *Dalton Trans.* **2017**, *46*, 2861−2873.
(97) Greif, A. H.; Hrobarik, P.; Kaupp, M. Insights into Trans-Ligand and Spin-Orbit Effects on Electronic Structure and Ligand NMR Shifts in Transition-Metal Complexes. *Chem. - Eur. J.* **2017**, DOI: 10.1002/chem.201700844.
(98) Gessner, V. H.; Meier, F.; Uhrich, D.; Kaupp, M. Synthesis and Bonding in Carbene Complexes of an Unsymmetrical Dilithio Methandiide: A Combined Experimental and Theoretical Study. *Chem. - Eur. J.* **2013**, *19*, 16729−16739.
(99) This interaction has been discussed as being C−C agostic in refs 57, 100, and 101.
(100) Suresh, C. H.; Baik, M.-H. α,β-(C-C-C) Agostic Bonds in Transition Metal Based Olefin Metathesis Catalyses. *Dalton Trans.* **2005**, *18*, 2982−2984.
(101) Etienne, M.; Weller, A. S. Intramolecular C-C Agostic Complexes: C-C Sigma Interactions by Another Name. *Chem. Soc. Rev.* **2014**, *43*, 242−259.
(102) Lauher, J. W.; Hoffmann, R. Structure and Chemistry of Bis(Cyclopentadienyl)-ML_n Complexes. *J. Am. Chem. Soc.* **1976**, *98*, 1729−1742.
(103) Albright, T. A.; Burdett, J. K.; Whangbo, M.-H. *Orbital Interactions in Chemistry*. 2nd ed.; Wiley VCH: Weinheim, 2013.
(104) Wiberg, K. B.; Hammer, J. D.; Zilm, K. W.; Cheeseman, J. R.; Keith, T. A. NMR Chemical Shifts. 1. The Role of Relative Atomic Orbital Phase in Determining the Sign of the Paramagnetic Terms: ClF, CH_3F, $CH_3NH_3^+$, FNH_3^+, and HC≡CF. *J. Phys. Chem. A* **1998**, *102*, 8766−8773.
(105) Arduengo, A. J.; Dixon, D. A.; Kumashiro, K. K.; Lee, C.; Power, W. P.; Zilm, K. W. Chemical Shielding Tensor of a Carbene. *J. Am. Chem. Soc.* **1994**, *116*, 6361−6367.
(106) Ziegler, T.; Folga, E.; Berces, A. A Density Functional Study on the Activation of Hydrogen-Hydrogen and Hydrogen-Carbon Bonds by Cp_2Sc-H and Cp_2Sc-CH_3. *J. Am. Chem. Soc.* **1993**, *115*, 636−646.
(107) Maron, L.; Perrin, L.; Eisenstein, O. DFT Study of CH_4 Activation by d^0 Cl_2LnZ (Z = H, CH_3) Complexes. *Dalton Trans.* **2002**, 534−539.
(108) Hoffmann, R. Building Bridges between Inorganic and Organic Chemistry (Nobel Lecture). *Angew. Chem., Int. Ed. Engl.* **1982**, *21*, 711−724.
(109) van de Heisteeg, B. J. J.; Schat, G.; Akkerman, O. S.; Bickelhaupt, F. Synthese von 1,3-Dimetallacyclobutanen mit dem Methylen-di-Grignardreagens. *J. Organomet. Chem.* **1986**, *308*, 1−10.
(110) Van de Heisteeg, B. J. J.; Schat, G.; Akkerman, O. S.; Bickelhaupt, F. Synthesis of 1,3-Metallatitanacyclobutanes of Group 4. *Organometallics* **1985**, *4*, 1141−1142.

DOI: 10.1021/acscentsci.7b00174
ACS Cent. Sci. 2017, 3, 759−768